Journal of Applied Polymer Science

Higher-Order Structural Analysis of Nylon-66 Nanofibers Prepared by Carbon Dioxide Laser Supersonic Drawing and Exhibiting Near-Equilibrium Melting Temperature

Toshinori Hasegawa,[1,2] Takumi Mikuni[2]

[1]Material Analysis Department, NISSAN ARC, LTD., 1 Natsushima-cho, Yokosuka, Kanagawa 237-0061, Japan

[2]Interdisciplinary Graduate School of Medicine and Engineering, University of Yamanashi, Takeda-4, kofu 400-8511, Japan

Correspondence to: T. Hasegawa (E - mail: hasegawa@nissan-arc.co.jp)

ABSTRACT: Extended chains and/or extended chain crystals (ECC) are important structures for improving the mechanical properties of polymer fibers. ECC have so far been produced using specially prepared materials or manufacturing methods. In our study on the production of nanofibers by carbon dioxide (CO_2) laser supersonic drawing, we succeeded in producing nylon-66 nanofibers having a high melting point near the equilibrium melting point (T_m^0). Two melting points (T_m) of 260 and 276°C were observed for the nanofibers, with the latter temperature being close to the T_m^0 (280°C) of nylon-66. A nanofiber that was heat treated at 279°C for 10 min displayed a large stacked lamellar structure with an average crystal thickness of 140 nm. That value was close to the average molecular chain length of 212 nm, which was calculated from the average molecular weight of the nanofibers. It was inferred from these results that ECC corresponding to the average molecular chain length were present in the nanofibers. The CO_2 laser supersonic drawing process is applicable to general purpose thermoplastic polymers and uses a simple drawing system. It is expected that this drawing method will help to improve the fundamental performance of general purpose polymers. © 2014 Wiley Periodicals, Inc. J. Appl. Polym. Sci. **2014**, *131*, 40361.

KEYWORDS: crystallization; differential scanning calorimetry (DSC); fibers; polyamides

Received 14 October 2013; accepted 30 December 2013

DOI: 10.1002/app.40361

INTRODUCTION

Both natural and synthetic nanofibers have been the object of vigorous research and development efforts. Products made of nanofibers with a fiber diameter of 1 μm or smaller have an exceptionally large specific surface area. A wide range of applications can be considered for such nanofibers, including clothing, filters, cell culture media and others, by making effective use of the tiny pores present between the fibers. It has been reported that the molecular chain orientation of fibers is heightened when the fiber diameter reaches the nanosize level, resulting in a marked improvement in physical properties such as electrical, mechanical and thermal characteristics.[1,2] At present, there are various methods of manufacturing nanofibers for industrial applications, including the sea-island conjugated melt spinning process[3] and the melt blowing process.[4] In recent years, the electrospinning process has also reached the stage of practical use in which the polymer material is melted in the solvent and spun into nanofibers in a high-voltage electric field.[5]

Suzuki et al. developed a carbon dioxide (CO_2) laser supersonic drawing method for producing long nanofibers in a single process that does not use any chemical solvents for which there is concern about their impact on the environment and living organisms. It has been reported so far that this new method of manufacturing nanofibers is applicable to the production of thermoplastic polymer nanofibers such as poly-L-lactide acid (PLLA),[6] polyethylene terephthalate (PET),[7,8] polyethylene naphthalate (PEN),[9] polyglycolic acid (PGA),[10] and polypropylene (PP)[11] nanofibers. With this drawing method, original fibers with a diameter of 100–200 μm are melted using a CO_2 laser and passed through a supersonic airflow such that the force of the air is utilized to accomplish supersonic drawing of nanofibers. The results of a flow analysis using a 3D finite element method showed that the spinning velocity at 346.5 m s^{-1} at 298.5 K is greater than the speed of sound and reaches a level three times faster than the ultrahigh-speed spinning velocity of 91–133 m s^{-1}.[12–14] Moreover, high-order structural changes not usually seen in ordinary fibers have been observed in nanofibers produced with this supersonic drawing method. For example, PET nanofibers[8] have exhibited multiple exothermic peaks of cold crystallization and endothermic peaks of melting. Attention is focused here on the temperature of the endothermic peaks.

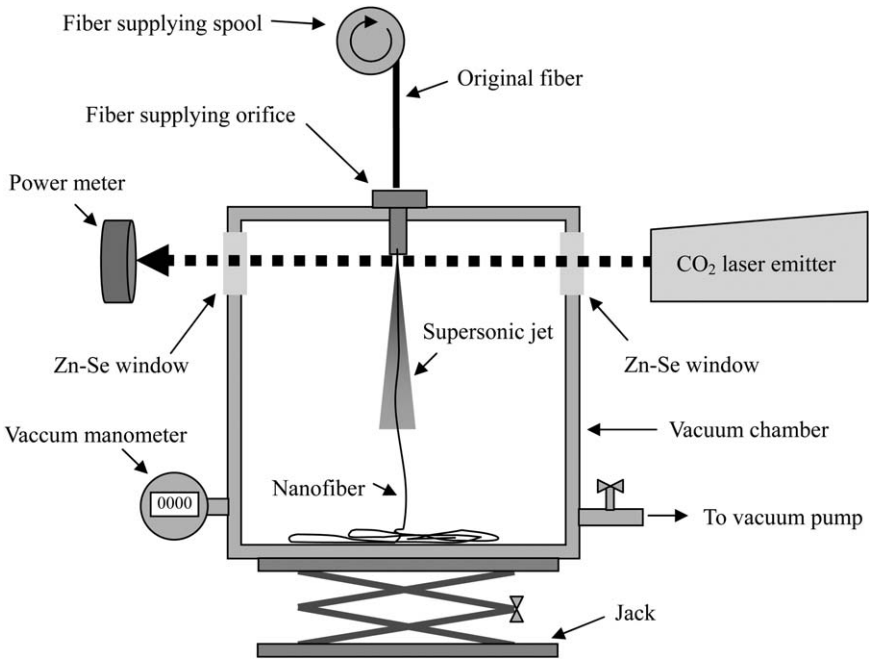

Figure 1. Schematic diagram of apparatus used for CO_2 laser supersonic drawing.

The endothermic peak on the high side is at 270°C, which is close to the equilibrium melting temperature T_m^0 of PET at 280°C.[15] This suggests the presence of thick crystals or extended-chain crystals (ECC) that grow in the direction of the molecular chains in the nanofibers.

Extended chains or ECC are important structures for improving the mechanical properties of polymer fibers. Numerous attempts have been made over the years to break up folded chain crystal (FCC) to form ECC. However, it has been difficult to produce fibers containing many ECC, with a few exceptions such as the gel spinning process using high-molecular-weight polyethylene (PE)[16] and the liquid crystal spinning process using rigid main-chain polymers.[17]

In our study on the production of nanofibers by CO_2 laser supersonic drawing, we discovered that nylon-66 nanofibers having a high melting point near T_m^0 (280°C)[18] can be manufactured with this process. This melting temperature suggests the presence of thick crystals or ECC that grow in the direction of the molecular chains in the nanofibers. It was postulated that elucidating the structure of the high-melting-point crystals might provide a clue for a method of improving the fundamental performance of general purpose polymers such as nylon, PET and others. Therefore, the present study focused on the high-melting-point crystals present in nylon-66 nanofibers produced by CO_2 laser supersonic drawing, and an investigation was made of their higher-order structures, including the microstructure, crystal structure and molecular chain length.

EXPERIMENTAL

Samples and Sample Preparation

Commercial nylon-66 pellets manufactured by Sigma–Aldrich were used as the raw material in this study. After drying the pellets under reduced pressure at 80°C for at least 24 h, they were melt-spun into the original fiber of 150–180 μm in diameter using a high-temperature, vacuum-gas-replacement, twin-rotor kneading and discharging machine made by Musashino Kikai. The melt spinning conditions were a spinning temperature of 285°C, fiber discharge rate of 6 mL min^{-1}, and a winding velocity of 145 m min^{-1}.

Figure 1 is a schematic diagram of the CO_2 laser supersonic drawing system used in producing the nanofibers.[6,7] This system consists of a spool for supplying the original fiber, a continuous-wave CO_2 laser emitter (wavelength: 10.6 μm, diameter: 1.8 mm), a vacuum chamber fitted with zinc selenide (ZnSe) windows, a 0.5 mm diameter orifice for supplying the original fiber to the vacuum chamber, a power meter and a vacuum pump.

Table I shows the 3D FEM flow analysis results for the flow velocity and temperature of the supersonic air jet emitted from the fiber supply orifice when the pressure in the vacuum chamber was reduced.[11] The data given in the table are the maximum velocity and minimum temperature in the velocity distribution and temperature distribution that occurred under each pressure condition in the chamber. The maximum velocity and minimum temperature were measured at a distance of <1 mm from exit of the fiber supply orifice.

Nanofibers were produced under fixed conditions of a laser power of 10 W, vacuum chamber pressure of 20 kPa and an orifice diameter of 0.5 mm while varying the laser beam position (χ) for irradiating the fiber exiting from the orifice. Figure 2 presents scanning electron microscope (SEM) micrographs and histograms of the diameter distribution of nanofibers produced at three χ positions of 0, 1, and 3 mm. Nanofibers produced at $\chi = 2$ mm, which resulted in the smallest average fiber diameter

Table I. Maximum Flow Velocity (v) and Minimum Temperature (T) of the Supersonic Air Jet Emitted from the Fiber Supply Orifice Under Four Different Chamber Pressures (P)

P (kP_a)	v (m s^{-1})	T (K)
50	324	247
30	446	200
20	530	164
10	619	109

Sonic speed (C) at 298.5 K: 346.5 m s^{-1}.

of 0.59 μm, were used as the samples for structural analysis in this study.

Differential Scanning Calorimetry

The melting point of the samples was measured by differential scanning calorimetry (DSC). The instrument used was a DSC-Q1000 differential scanning calorimeter made by TA Instruments. A 0.5 mg sample was measured in a temperature range of −10–310°C at a temperature rise rate of 10°C min^{-1}. To prevent oxidation of the samples during the measurement, nitrogen gas was injected into the sample chamber at a flow rate of 100 mL min^{-1}. The maximum value of the endothermic melting peak was defined as the melting point in this study.

Transmission Electron Microscopy

The sample microstructure was observed by transmission electron microscopy (TEM). After samples were embedded in epoxy resin such that the sectioning direction and fiber axis were parallel, they were trimmed with a glass knife and then fixed in a Leica Ultracut S ultramicrotome. Samples were sectioned into slices of 50–70 nm in thickness using a diamond knife at a temperature of −80°C and a speed of 0.2 mm s^{-1}. The ultrathin sections thus obtained were placed on a 100 mesh grid and immersed in a 10% phosphotungstic acid solution for 15 min before being stained. The stained sections were then observed using a Hitachi H-800 TEM operated at an accelerating voltage of 200 kV.

Wide-angle X-ray Diffraction

The crystal structure of the samples was measured by wide-angle X-ray diffraction (WAXD). The instrument used was a Bruker AXS D8 Discover with GADDS microdiffractometer fitted with a Vantec 200 X-ray detector and a heating stage. A sample of ~5 mg was sandwiched between high-purity aluminum foil and fixed to the heating stage. The X-ray source was Cu Kα ($\lambda = 0.154$ nm), the voltage was 45 kV, the current was 110 mA, and the detector used was a Vantec 2000 2D detector. The camera length was 20 cm, and measurements were made for 3 min in a temperature range of 30–300°C. Nitrogen gas was injected into the sample chamber at a flow rate of 300 mL min^{-1} to prevent oxidation of the samples during measurement.

Size Exclusion Chromatography

The molecular weight distribution of the samples was measured by size exclusion chromatography (SEC). The instruments used were a Waters GPC-14 gel permeation chromatograph and a Waters RI-2414 differential refractive index detector. One Shodex HFIP-LG column and two HFIP-806M columns were used with the column temperature set at 40°C. Hexafluoroisopropanol, to which 5 mM of trifluoroacetic acid sodium was added, was passed through the column as a mobile phase at a flow rate of 0.5 mL min^{-1}. The sample concentration was adjusted to ~0.06 wt/v %, and the solution used was strained with a membrane filter having a pore size of 0.45 μm. The molecular weight distribution of the nylon-66 was measured directly using as a reference sample nylon-66 with a weight average molecular weight of 36,500 and ε-caprolactam having a molecular weight of 113.

RESULTS AND DISCUSSION

Melting Temperature of Nylon-66 Nanofibers

The DSC curves obtained for the original fiber and an as-drawn nanofiber before heat treatment are shown in Figure 3(a,b), respectively. The original fiber showed nearly a single melting peak at a maximum temperature of 258°C, whereas the as-drawn nanofiber displayed two melting peaks at 261 and 276°C. The peak at the lower temperature of 261°C is the T_m generally observed for nylon-66. The peak at the higher temperature of 276°C is near the T_m^0 (280°C) of nylon-66.[18]

Schreiber and Phillips reported that the high-temperature melting peaks often seen in the DSC curves of nylon 66 are due to recrystallization during melting.[19] This suggests that imperfect crystals or small crystals were present in the samples examined. Therefore, the nylon-66 nanofibers produced in this study were subjected to a heat treatment process in an effort to produce larger crystals by increasing the degree of perfection of the crystals in the fibers. As a result of investigating the heat treatment temperature, the heat treatment was performed at 279°C for 10 min, which was the highest temperature at which the nanofibers did not melt.

The DSC curve obtained for a nanofiber heat-treated at 279°C for 10 min is shown in Figure 3(c). The heat treatment was performed inside the DSC sample chamber on a nanofiber sandwiched between aluminum pans. The heat-treated nanofiber also displayed two melting peaks at 259 and 279°C. Compared with the results before the heat treatment, the two peaks were completely separated, and the melting peak at the higher temperature of 279°C approached the T_m^0 value of 280°C. This melting behavior induced by the heat treatment indicates that the crystals present in the as-drawn nanofiber were imperfect or small in size.

T_m^0 of Nylon-66

The Gibbs–Thomson equation shown in eq. (1) below is a widely used method of determining the T_m^0 of polymer crystals.

$$T_m = T_m^0\left(1-\frac{2\gamma}{l\Delta H_m}\right) \quad (1)$$

where γ is the specific surface free energy of lamellar crystals, ΔH_m is the heat of fusion of crystals, and l is the crystal thickness. It has been reported that the values of l for nylon-66 when $T_m = 247$°C and $T_m = 260$°C are 5.4 and 9.5 nm, respectively.[18] Figure 4 shows the Gibbs–Thomson plot. From this figure, T_m^0 of 280°C and γ of 60 erg cm^{-2} were obtained for nylon-66.

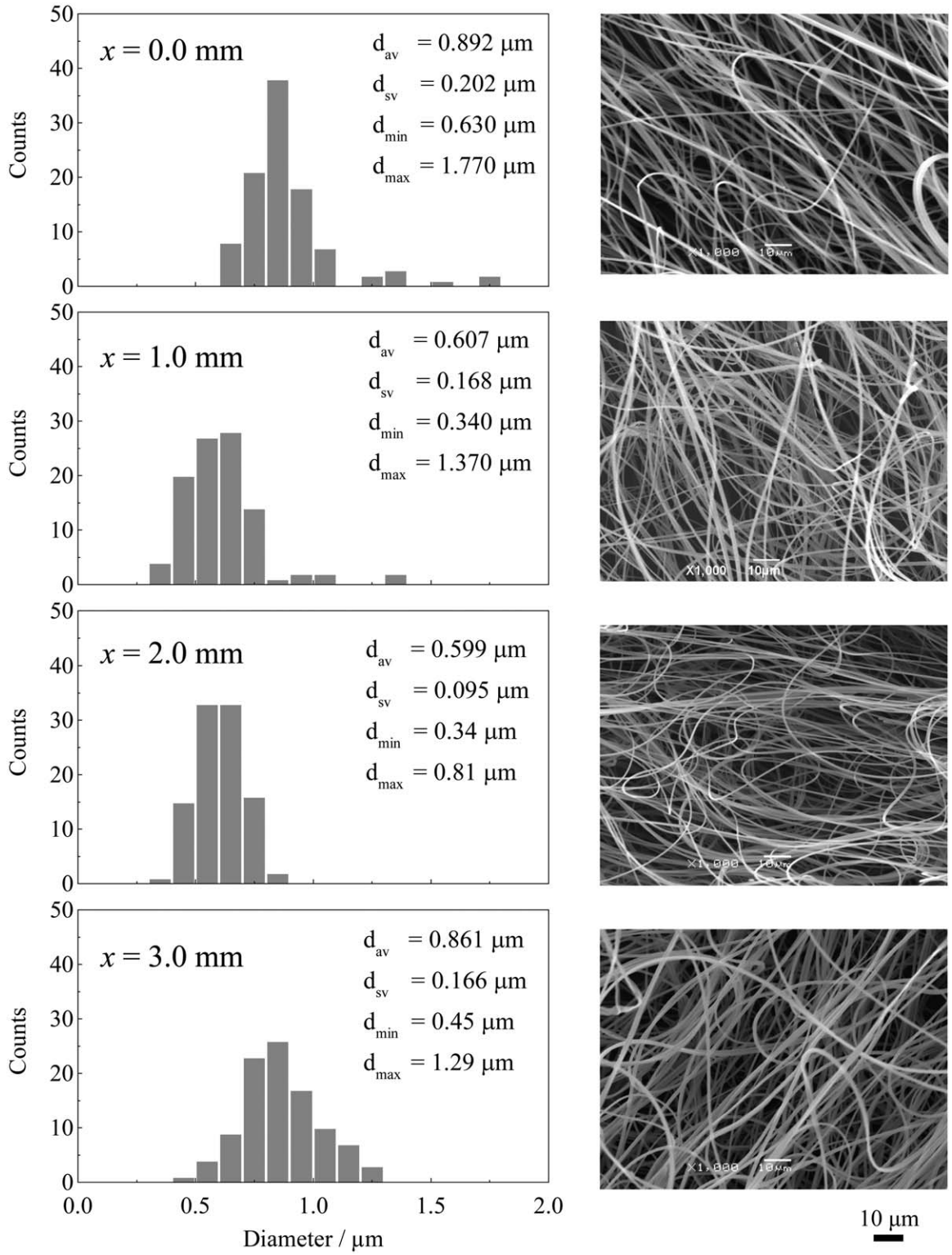

Figure 2. Histograms showing the diameter distribution of nylon-66 nanofibers and SEM micrographs at a magnification of 1000 obtained at four different laser beam irradiation positions (x).

Using the data in Figure 4, the measured T_m value can be converted to an equivalent l value. For the as-drawn nanofiber, l was ~9 nm for $T_m = 262°C$ and ~43 nm for $T_m = 276°C$. For the nanofiber heat-treated at 279°C for 10 min, l was ~8 nm for $T_m = 259°C$ and ~170 nm for $T_m = 279°C$. These results imply that thick crystals were present in the nanofibers examined in this study. Other T_m^0 values reported for nylon-66 besides 280°C include 275.7°C,[20] 301°C,[21] and 303.7°C.[19] This

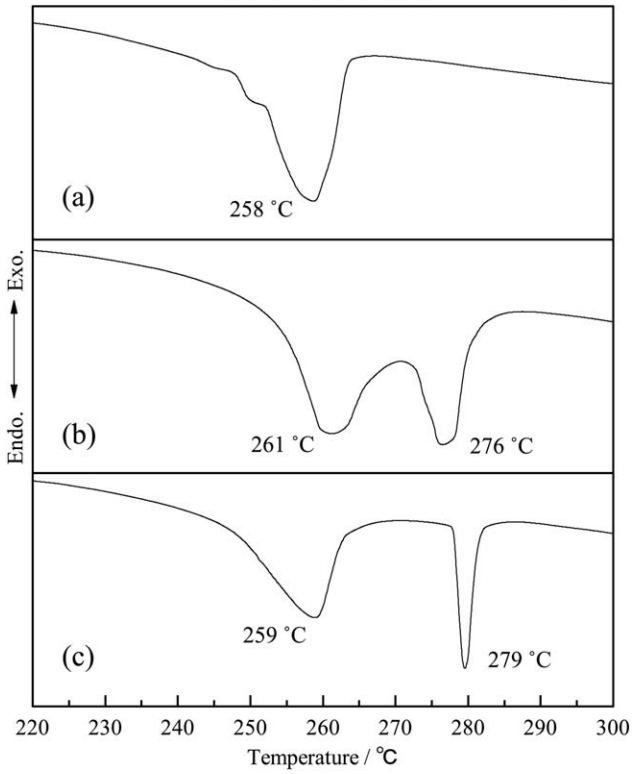

Figure 3. DSC curves of (a) original fiber, (b) as-drawn nanofiber, and (c) nanofiber heat-treated at 279°C for 10 min.

temperature variation signifies the difficulty of measuring T_m^0 of polymer crystals consisting of long molecular chains as compared with low-molecular-weight crystals.

Microstructure of Nylon-66 Nanofibers

The Gibbs–Thomson plot is a method that is applied to crystals produced in an equilibrium state from a quasi-equilibrium state, such as lamellar crystals that are crystallized at a constant temperature over a long period of time. In contrast, the nanofibers investigated in this study were produced in a nonequilibrium state due to the drawing and heat treatment processes. For that reason, it would be unsuitable to apply this method to these nanofibers. Moreover, during the DSC process used to measure T_m, the measured T_m values may fluctuate due to reorganization or superheating of the sample during the measurement. To avoid such uncertain factors, an attempt was made to measure l based on a TEM observation of the nanofiber microstructure. Yamada et al. used a TEM to measure the thickness of lamellar crystals of samples that had been prepared for the purpose of determining the T_m of isotactic polypropylene accurately. They reported that the thickness of the lamellar crystals increased as the melting peak rose to a high temperature level.[22]

Figure 5 presents TEM micrographs of (a) the original fiber, (b) the as-drawn fiber and (c) the nanofiber heat-treated at 279°C for 10 min. The original fiber displays a spherulite structure in which it is observed that lamellar crystals of 7 nm in thickness grew from the central core. The microstructure of the as-drawn nanofiber before heat treatment cannot be observed because the entire fiber was stained. In contrast, the heat-treated nanofiber

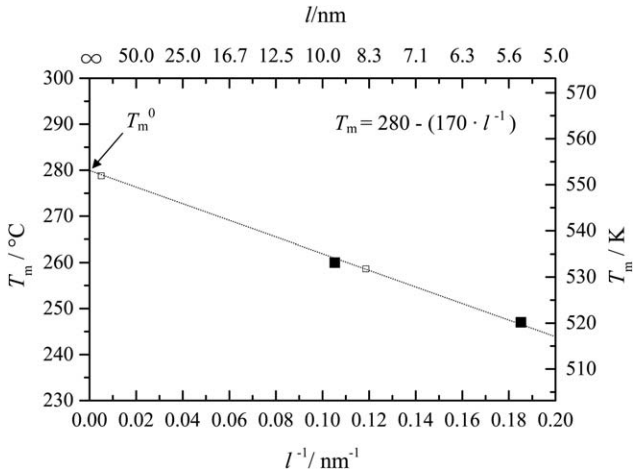

Figure 4. Gibbs–Thomson plot, T_m vs. l-1 of nylon-66.

exhibits a stacked lamellar structure that grew in the axial direction of the fiber. Figure 6 shows a typical histogram of the crystal thickness, l, measured from the TEM micrograph of the nanofiber heat-treated at 279°C for 10 min. The crystal thickness is worthy of attention here. The average crystal thickness (l_{av}) was 140 nm, the minimum crystal thickness (l_{min}) was 21 nm, and the maximum crystal thickness (l_{max}) was 313 nm. The l_{av} value of 140 nm was close to the l value of 170 nm found from the T_m in the Gibbs–Thomson plot in Figure 4.

Crystal Structure of Nylon-66 Nanofibers

Wide-angle X-ray diffraction (WAXD) measurements were made of the nanofibers because T_m is also influenced by the crystal structure and other factors in addition to l. Figure 7 shows WAXD profiles of (a) the original fiber, (b) the as-drawn nanofiber and (c) the nanofiber heat-treated at 279°C for 10 min. The original fiber displayed diffraction peaks at $2\theta = 20.3°$ (d_{100}) and at 23.4° ($d_{010/110}$) attributable to the triclinic structure (α-form).[23] Diffraction peaks are seen at $2\theta = 20.3°$ (d_{100}) and at 22.8° ($d_{010/110}$) for the as-drawn nanofiber, and the broad shape of the peaks implies an imperfect crystal structure. The heat-treated nanofiber exhibited diffraction peaks at $2\theta = 20.3°$ (d_{100}) and at 23.8° ($d_{010/110}$) attributable to the α-form.

Figure 8 shows the temperature dependence of the d-spacing found for (a) the original fiber, (b) the as-drawn fiber and (c) the heat-treated fiber when they were heated from 30 to 300°C. It is known that the crystal structure of nylon-66 at room temperature is the α-form in which hydrogen-bonded sheets are arranged in a hierarchy; upon heating, nylon-66 undergoes the Brill transition and the crystal structure changes to a pseudo-hexagonal structure (β-form) with the hydrogen bonds arranged on different levels.[24,25] In the original fiber, the d-spacing between d_{100} and $d_{010/110}$ of the α-form narrowed as the temperature rose, a transition to the β-form occurred near 137°C, and that structure was subsequently observed until 252°C. That temperature almost coincides with the T_m of nylon-66. For the as-drawn nanofiber, the transition to the β-form occurred near 113°C, and that structure then continued until 266°C. Because of the imperfect crystal structure of the as-drawn nanofiber, the transition temperature to the β-form was lower, but heating

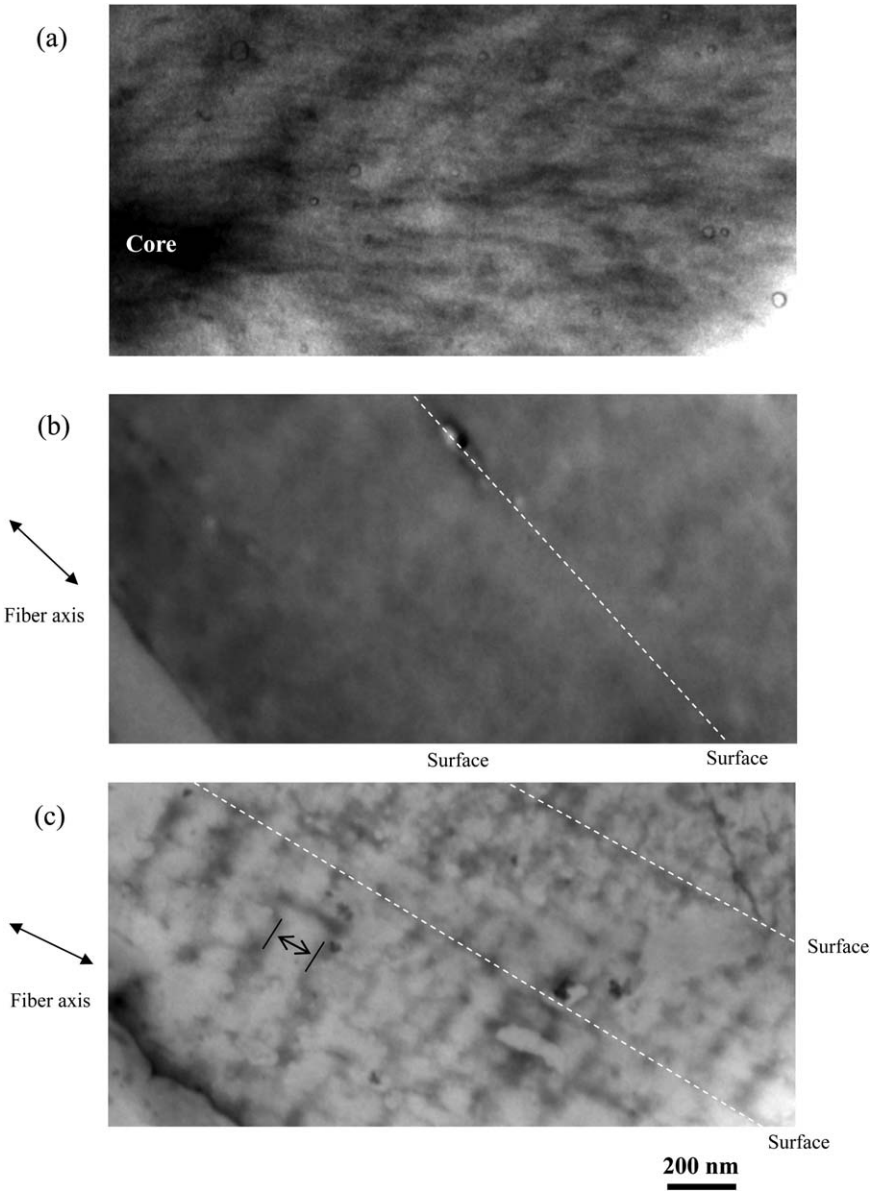

Figure 5. TEM micrographs of (a) original fiber, (b) as-drawn nanofiber, and (c) nanofiber heat-treated at 279°C for 10 min.

probably induced crystal reorganization, causing T_m to rise to a higher level. In contrast, the nanofiber heat-treated at 279°C for 10 min underwent a transition to the β-form at a higher temperature near 198°C and crystals were observed until 272°C. For all of the nanofiber samples, the β-form was the only crystal structure seen until near the melting point. The foregoing results presumably indicate that the T_m observed for the nanofibers on the high temperature side was not due to differences in the crystal structure.

Molecular Chain Length of Nylon-66 Nanofiber

It was predicted from the DSC, TEM and WAXD results that ECC were present in the heat-treated nanofiber. To verify that, the molecular chain length (Ml) was investigated. Using the peak molecular weight (M_p) measured by size exclusion chromatography (SEC), Ml was calculated with eqs. (2) and (3) below.

$$n = {}^{M_p}/_{262} \tag{2}$$

$$Ml = n \times 1.72 \tag{3}$$

where n is the degree of polymerization, 262 is the unit molecular weight of nylon-66, and 1.72 is the fiber identity period. Figure 9 shows the SEC curve found for the nanofiber heat-treated at 279°C for 10 min. The molecular weight was distributed in a range of about 1000 to about 200,000 with a peak at ~34,000.

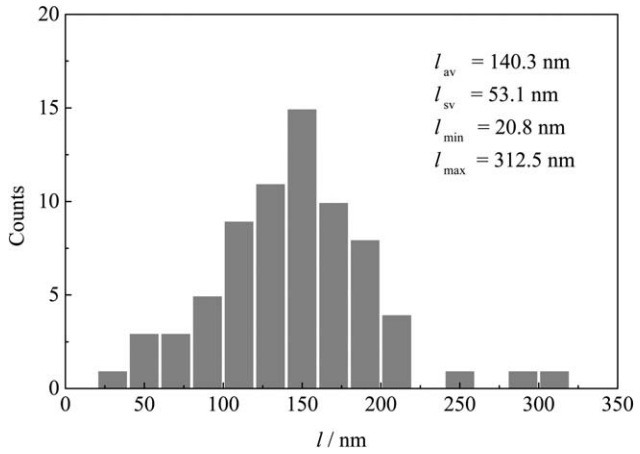

Figure 6. Typical histogram of l of nylon-66 nanofiber heat-treated at 279°C for 10 min.

The Ml values are also plotted in the graph. The Ml values for M_p values of 34,000, 200,000, and 1000 were 212, 1312, and 6.6 nm, respectively. These values nearly coincide with the range of crystal thickness measured from the TEM observations. This presumably indicates that ECC corresponding to these molecular chain lengths were present in the nylon-66 nanofibers examined in this work.

CONCLUSIONS

1. A T_m value of 276°C was observed for the nylon-66 nanofibers, which was close to $T_m^0 = 280$°C.

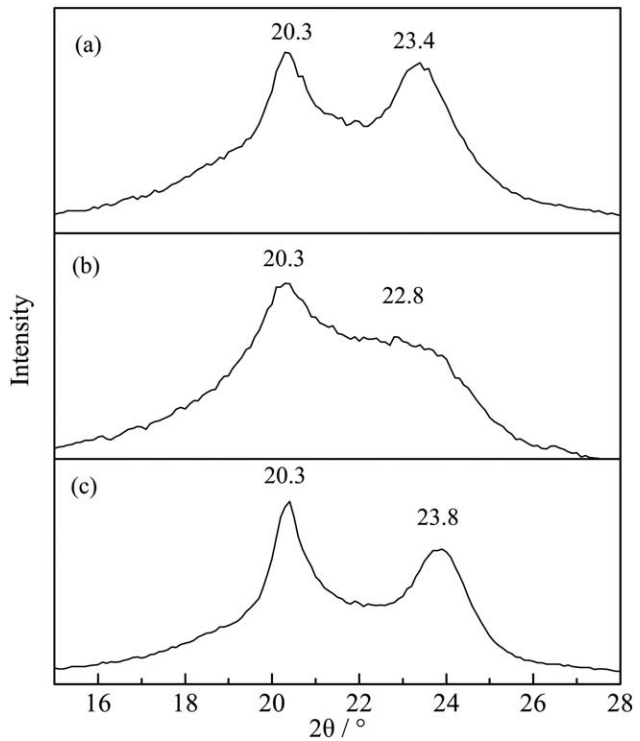

Figure 7. WAXD profiles for (a) original fiber, (b) as-drawn nanofiber, and (c) nanofiber heat-treated at 279°C for 10 min.

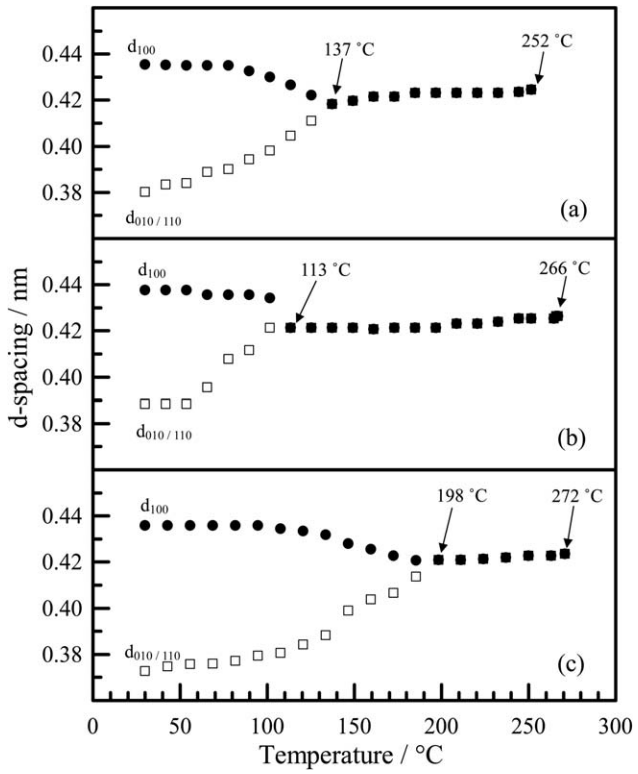

Figure 8. Temperature dependences of d-spacing for (a) original fiber, (b) as-drawn nanofiber, and (c) nanofiber heat-treated at 279°C for 10 min.

2. The crystals present in the as-drawn nanofiber had an imperfect structure, but the application of a heat treatment process presumably induced crystal reorganization that caused T_m to rise.
3. The nanofiber heat-treated at 279°C for 10 min developed a stacked lamellar structure that grew in the fiber axial direction and the average crystal thickness was 140 nm.
4. An average molecular chain length of about 212 nm was calculated from the average molecular weight of the nanofibers.

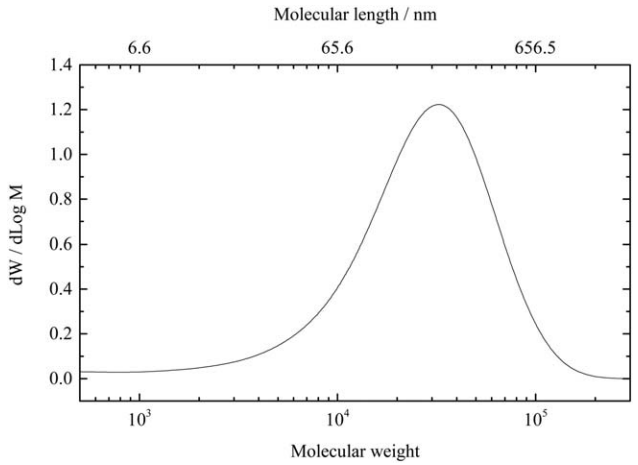

Figure 9. SEC curve of nanofiber heat-treated at 279°C for 10 min.

5. The foregoing results presumably indicate the presence of extended chain crystals corresponding to the molecular chain length in the nylon-66 nanofibers produced by CO_2 laser supersonic drawing.

ACKNOWLEDGMENTS

The authors thank Professor Akihiro Suzuki of the University of Yamanashi and Kei Kubobuchi, Mayumi Gonda, and Dr. Atsushi Kato of NISSAN ARC, Ltd. for their invaluable cooperation with this study. Thanks are also due to Yuichi Ishikawa and Naoyuki Takimoto of Musashino Kikai Co., Ltd. and Toray Research Center, Inc. for their cooperation with the sample preparation and SEC measurements.

REFERENCES

1. Kakade, M. V.; Givens, S.; Gardner, K.; Lee K. H.; Chase, D. B.; Rabolt, J. F. *J. Am. Chem. Soc.* **2007**, *129*, 2777.
2. Catalani, L. H.; Collins, G.; Jaffe, M. *Macromolecules* **2007**, *40*, 1693.
3. Kamiyama, M.; Soeda, T.; Nagajima, S.; Tanaka, K. *Polym. J.* **2012**, *44*, 987.
4. Borkar, S.; Gu, B.; Dirmyer, M.; Delicado, R.; Sen, A.; Jackson, B. R.; Badding, J. V. *Polymer.* **2006**, *47*, 8337.
5. Reneker, D. H.; Chun, I. *Nanotechnology* **1996**, *7*, 216.
6. Suzuki, A.; Aoki, K. *Eur. Polym. J.* **2008**, *44*, 2499.
7. Suzuki, A.; Tanizawa, K. *Polymer* **2009**, *50*, 913.
8. Suzuki, A.; Arino, K. *Polymer* **2010**, *51*, 1830.
9. Suzuki, A.; Yamada, Y. *J. Appl. Polym. Sci.* **2010**, *116*, 1913.
10. Suzuki, A.; Shimizu, R. *J. Appl. Polym. Sci.* **2011**, *121*, 3078.
11. Suzuki, A.; Arino, K. *Eur. Polym. J.* **2012**, *48*, 1169.
12. Gang, W.; Hongwei, L.; Yiqun, W.; John, A. *Polymer* **2002**, *45*, 4915.
13. Miyake, K.; Ito, H.; Kikutani, T.; Okui, N. *J. Polym. Eng.* **1966**, *19*, 395.
14. Young-Pyo, J.; Christopher, L. C. *J. Eng. Fibers Fabrics.* **2009**, *4*, 34.
15. Wunderlich, B. Thermal Analysis of Polymeric Materials; Springer: Berlin, **2005**; p 628.
16. Smith, P.; Lemstra, P. J.; Kalb, B.; Pennings, A. *J. Polym. Bull.* **1979**, *1*, 733.
17. Stuart, M. L. Handbook of Composite Reinforcements; Wiley: California, **1993**; p 5.
18. Wunderlich, B. Macromolecular Physics; Academic Press: New York, **1980**; Vol. *3*, p 161–162.
19. Schreiber, L. S.; Phillips. P. *J. Eur. Polym. J.* **2007**, *43*, 1933.
20. Kamide, K.; Higashinakagawa, F. *Netsusokutei* **1978**, *5*, 63.
21. Qui, W.; Habenschuss, A.; Wunderlich, B. *Polymer* **2007**, *48*, 1641.
22. Yamada, K.; Hikosaka, M.; Toda, A.; Yamazaki, S.; Tagashira, K. *Macromolecules* **2003**, *36*, 4802.
23. .Bunn, C. W.; Garner, E. V. *Proc. R. Soc.* **1947**, *A189*, 39.
24. Brill, R. *J. Prakt. Chem.* **1942**, *161*, 49.
25. Ramesh, C.; Keller, A.; Eltink, S. J. E. A. *Polymer* **1994**, *35*, 2483.